Residual stresses in spot welded new generation aluminium alloys
Part B – finite element simulation of residual stresses in a spot weld in 5754 aluminium alloy

X. Long and Sanjeev K. Khanna*

An incremental thermo-electrical-mechanical coupled finite element model has been developed for predicting the residual stress field in a 5754 aluminium alloy spot welded joint. The complete spot welding process, including squeezing, welding, holding and cooling cycles, as well as the temperature and stress histories during those cycles in the welded joint have been investigated. All the required thermo-physical and thermo-mechanical properties used were experimentally measured. The results show that tensile residual stress predominates the spot nugget area. The highest tensile residual stress, with a value close to the material's yield strength, occurs around the centre of the nugget. The residual stress value decreases slightly towards the edge of the spot nugget.

Keywords: New generation aluminium alloys, Spot welding, Residual stresses, Thermo-electrical-mechanical FEM

Introduction

Aluminium alloys are being actively considered as substitute materials for steel in the automotive industry. This substitution is being propelled by the need for greater fuel economy in automobiles. Theoretical calculations based on conventional automotive designs have estimated that a 40% reduction in body weight can possibly increase fuel efficiency by over 7%.[1] In addition, the evolution of advanced metallurgy technology has led to the development of new aluminium alloys with higher strength-to-weight ratio, better weldability, enhanced formability, and improved corrosion resistance relative to conventional aluminium alloys.[2]

Although some new welding techniques have been used to manufacture automotive structures, such as laser beam welding[3,4] and friction stir welding,[5–7] electrical resistance spot welding (or spot welding) is still a major method of joining sheet metal in the automotive industry. Spot welding joins metal parts together with a localised, permanently bonded connection. Compared with other welding processes, resistance spot welding is fast, easily automated and easily maintained. Figure 1 shows a schematic diagram of the spot welding setup. The application of the appropriate squeezing pressure, results in the formation of a contact interface between the two workpieces or sheets. Then a high electric current is passed that results in localised melting of the metal sheets between the electrodes. When electric current is turned off, molten metal cools down and solidifies under the pressure of the electrodes, resulting in the formation of a spot weld nugget. The electrodes are then retracted. When the welded region cools down, residual stresses are generated as a result of the local heterogeneous thermal cycle, heterogeneous thermo-plastic deformation, and some phase transformation induced by plastic deformation (i.e. phase transformation induced deformation). Residual stresses significantly affect stress corrosion cracking and hydrogen-induced cracking and also fatigue strength in these weldments.[8]

As a result of the complexity involved in the measurement of residual stresses, there has been an increasing use of numerical simulation procedures for estimating or predicting residual stress in weldments.[9] However, previous numerical simulations on spot welding have mainly focused on the temperature distribution, nugget growth, electrode design, welding parameters' optimisation, etc.[10–14] The complete welding process simulation for residual stress prediction has not been investigated. To study residual stresses in a spot welded joint, however, the whole welding process, which includes squeezing cycle, welding (heating) cycle, holding cycle, and cooling cycle, should be considered in the simulation.

Since spot welding is a strongly coupled process that cannot be solved directly by commercial software, a

Department of Mechanical and Aerospace Engineering, University of Missouri – Columbia, Columbia, MO 65211, USA

*Corresponding author, email Khannas@missouri.edu

Published by Maney on behalf of the Institute
Received 8 July 2003; accepted 8 January 2004
DOI 10.1179/174329305X29483

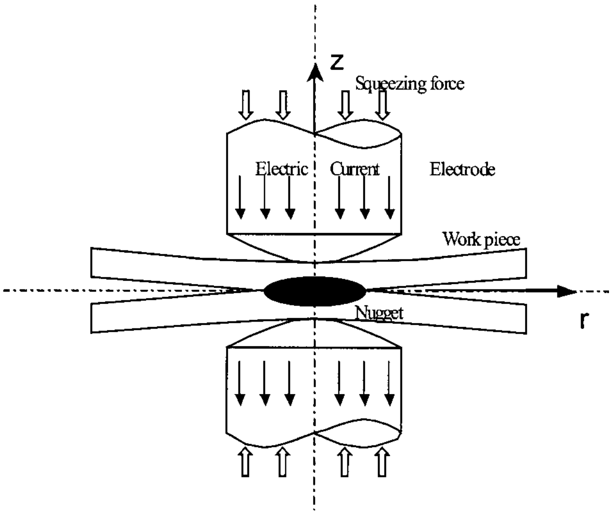

1 Schematic diagram of spot welding setup

sequentially coupled finite element model was used in previous investigations.[14,15] The sequentially coupled model simulates the temperature field and stress field in the spot weld in a sequential order. Under this condition, the contact radii between the electrode/workpiece and faying interface are assumed to remain constant during the whole welding process. This is not actually true because contact radii are the result of competition between thermal expansion and electrode squeezing force, thus they vary during the welding process. Later, an incrementally coupled thermal-electro-mechanical model was developed.[11–14] In the coupled thermal-electro-mechanical model, at predetermined small time increments, the contact radii from thermo-mechanical analysis are input to the electrical-thermal analysis as electrical and thermal boundary conditions. Then the temperature distribution from electrical-thermal analysis is input to the thermo-mechanical analysis as a body load. This iterative procedure is applied during the whole welding process. Since the simulated contact condition at the electrode/workpiece and faying interface is closer to the true contact status, this incrementally coupled model leads to more accurate results compared with the previous sequential coupled model.

In the present study, an incrementally coupled finite element model has been established to study the complete spot welding process, and temperature dependent physical and mechanical material properties determined in Part A[16] have been used. The material that has been investigated is 5754 aluminium alloy. The chemical composition of 5754 aluminium is shown in Table 1.[17] The history of internal stress generation and the final residual stress distribution in the spot welded aluminium joint have been obtained. The growth of the spot weld nugget has also been studied.

Table 1 Chemical composition of 5754 aluminium alloy, wt-%

Si	Fe	Cu	Mn	Mg	Cr	Zn	Ti
0·40	0·40	0·10	0·50	2·6–3·6	0·30	0·20	0·15

Finite element model and analysis

Modelling the spot welding process

The spot welding process can be divided into four cycles as explained below:

(i) Presqueezing cycle: workpieces are deformed under a presqueezing force, which develops a good workpiece/workpiece, workpiece/electrode contact. The presqueezing cycle is followed immediately by the heating cycle.
(ii) Heating cycle: workpieces are heated by passing current, while the squeezing force is kept constant.
(iii) Holding cycle: current is cut off but the squeezing force is maintained. The workpieces start cooling.
(iv) Cooling cycle: squeezing force is removed. The spot welded joint and workpiece cool down to room temperature. Residual stresses are developed in the welded joint.

It can be seen that the spot welding process involves a complex coupling among thermal, electrical and mechanical induced deformation processes. Since such a strongly coupled model cannot be solved directly by commercially available software, an incremental method has been adopted using APDL (ANSYS Parametric Design Language) in ANSYS commercial software. First, a solid element is used to analyse the initial contact radius (between the electrode/workpiece and the workpiece/workpiece) in the model. Then a thermo-electrical coupled element is used to analyse the temperature field in the same model. The contact information from thermo-mechanical analysis is input to the thermo-electrical analysis to determine the electrical potential distribution. After that, the thermo-mechanical solution is carried out. The temperature field from the former thermo-electrical analysis is input as a body load. After finishing the thermo-mechanical analysis, new contact information is gained. Over a given time increment, the interactions between the electrical-thermal and thermo-mechanical analysis are obtained. This iterative procedure is applied during the whole welding cycle. A time increment of 0·001 s was used to ensure sufficient accuracy and good calculation convergence. During the holding cycle, the current is set to zero, and convection is the only thermal load in the thermo-electrical model. In the cooling cycle, the electrode is separated (non-contact), and convection is still the only thermal load in the thermo-electrical model. The condition in the thermo-mechanical model is a little complicated because a stress release and a re-equilibrium process occurs in the workpieces after separation of the electrodes. The internal stresses continually change during cooling of the workpieces in the thermo-electrical model. When the temperature decreases to near ambient temperature (25°C), the calculated internal stress distribution in the thermo-mechanical model is the residual stress in the spot welded joint. This simulation process is schematically shown in Fig. 2.

Geometric model

Dome type electrodes are typically used in aluminium and aluminium alloy spot welding. Because of symmetry, only one-quarter of the model is analysed in the

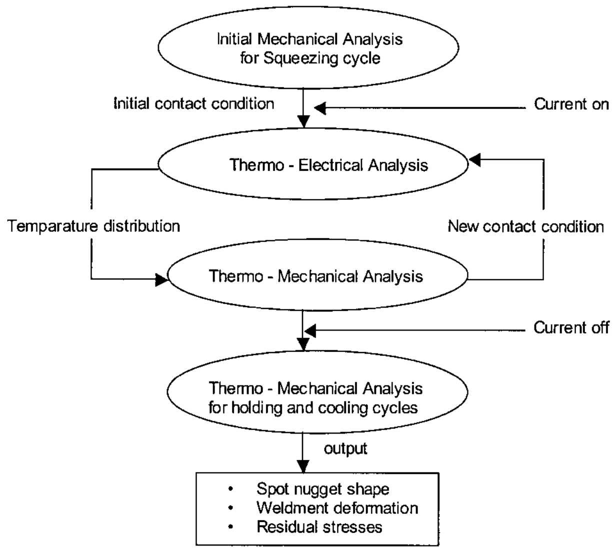

2 Flow chart for finite element based simulation of spot welding process

axisymmetric problem of spot welding, which is shown in Fig. 3. The mesh divisions in the finite element analysis (FEA) for thermo-electrical analysis and thermo-mechanical analysis are shown in Fig. 4. The mesh in thermo-electrical analysis contains 995 elements, whereas there are 2815 elements (which includes 1940 contact elements) in the thermo-mechanical analysis. A more dense mesh was used in the spot nugget forming area, which has a higher temperature gradient (and therefore higher stress gradient) than anywhere else.

It can be seen that the mesh for thermo-electrical analysis shown in Fig. 4 is a little different from that for thermo-mechanical analysis. This is because no contact element is available for thermo-electrical analysis as in the case of thermo-mechanical analysis. Thus a death and birth technique was used to simulate the contact and separation condition in thermo-electrical analysis, as shown in Figs. 4*a* and 5. The death and birth of elements in thermo-electrical analysis is controlled by the contact information from thermo-mechanical analysis. The contact condition between the faying surfaces in thermo-electrical analysis can be simulated by setting the thermo-electrical model boundary values, which is also controlled by the contact information from thermo-mechanical analysis.

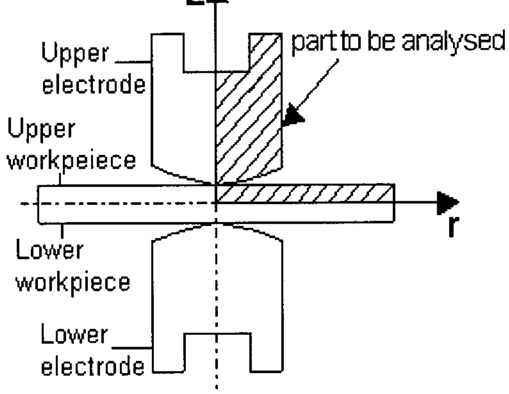

3 Part to be analysed in symmetric model

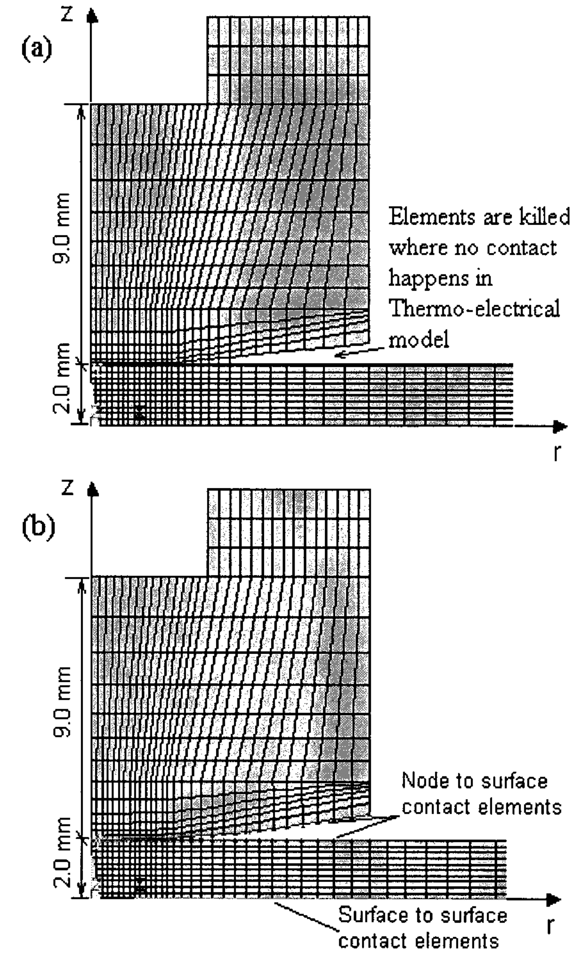

4 FEM mesh for *a* thermo-electrical analysis and *b* thermo-mechanical analysis

In Fig. 4*b*, it may be seen that there are two kinds of contact elements used. One is node to surface contact element, which is for simulating the contact condition between the dome shaped electrode and the workpiece. The second is a surface to surface contact element, which simulates the contact condition between the two faying surfaces (i.e. workpiece to workpiece).

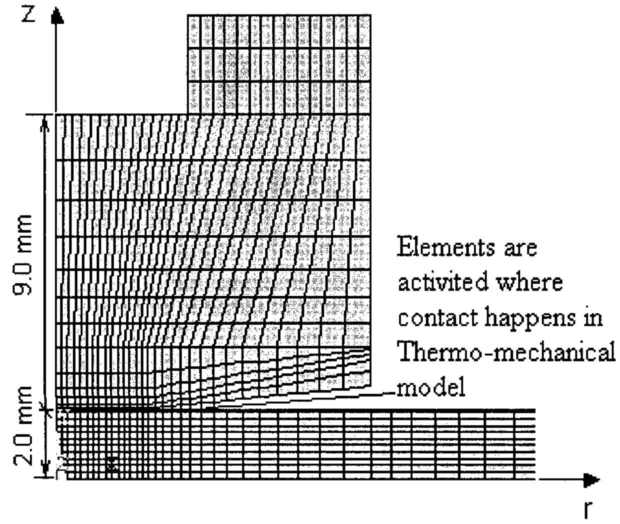

5 Contact condition after elements become death in thermo-electrical analysis

Basic theory

All the equations in the present study are based on the cylindrical coordinate system, as shown in Fig. 4. The governing equation for calculation of the electrical potential φ in the whole model is

$$\frac{\partial}{\partial r}\left(\sigma\frac{\partial\varphi}{\partial r}\right)+\frac{\sigma}{r}\frac{\partial\varphi}{\partial r}+\frac{\partial}{\partial z}\left(\sigma\frac{\partial\varphi}{\partial z}\right)=0 \tag{1}$$

where r is the radial distance in this column coordinate system, z is the distance in the axis direction of the coordinate system, and σ is the electrical conductivity. By solving equation (1), the electrical potential φ is obtained. According to the electric current heat generation (q) rule

$$q=I^2Rt \tag{2}$$

where I is the current, R is the material electrical resistance, and t is the time for which current is passed. Since $I=\varphi/R$, equation (2) can be rewritten as

$$q=\phi^2 t/R \tag{3}$$

The governing equation for transient temperature field distribution, which involves electrical resistance heat can be written as

$$\rho c\frac{\partial T}{\partial t}=\frac{\partial}{\partial r}\left(k\frac{\partial T}{\partial r}\right)+\frac{k}{r}\frac{\partial T}{\partial r}+\frac{\partial}{\partial z}\left(k\frac{\partial T}{\partial z}\right)+q \tag{4}$$

where ρ is the material's density, c is heat capacity, T is temperature, t is time, and k is the thermal conductivity. The material properties c, k and σ are temperature dependent. Substituting equation (3) in (4), and solving the resultant equation, the temperature distribution generated by passing electric current is obtained.

For stress and strain analysis, the governing finite element equation is

$$H\cdot\boldsymbol{\Phi}+\boldsymbol{f}=0 \tag{5}$$

where $\boldsymbol{\Phi}$ is the vector of unknown displacements, $\boldsymbol{f}$ is the vector of loads and H is the stiffness matrix. Since residual stress is caused by heterogeneous plastic deformation of the material, temperature dependent mechanical properties of the material were used.[16] The plastic deformation of the material was modelled using the bilinear kinematic hardening (BKIN) option in the ANSYS program, which assumes the total stress range is equal to twice the yield stress and the work hardening is linear.

Boundary conditions and material properties

Electrical boundary conditions

In the welding cycle, a root-mean-square (rms) value of total alternating current was applied uniformly at the top of the copper electrode. At the faying surface of the workpieces, the voltage of the nodes was set to zero if the nodes were under contact according to the contact information from thermo-mechanical analysis.

Welding conditions

For the 5754 aluminium alloy, the value of ac welding current used was 8000 A rms, with a duration of three cycles (0·05 s) for preheating; 29 000 A, with duration of three cycles (0·05 s) for welding; and 32 000 A, with duration of five cycles (0·083 s) for post-heating. The holding cycle had a time duration of 0·168 s, and the cooling cycle had a time duration of 150 s. A squeeze force of 7500 N was used. The dome shaped electrode had a radius of 50·8 mm. The thickness of both aluminium sheets used was 2·0 mm.

Thermal boundary conditions

The temperature at the water cooling cavity was restrained to 25°C, and convection heat transfer to ambient air was specified on all the lateral surfaces of the electrode and workpiece that are not in contact. The coefficient of heat transfer was set to 12 W m^{-2} K^{-1}.[18]

Mechanical boundary conditions

Uniform pressure was applied at the top of the copper electrode during welding and holding cycles. The electrode was retracted at the end of the holding cycle. In the cooling cycle, some contact elements at the faying surface, where the highest temperature reached is the melting point of the material, were set to always contact because of the solidification of liquid metal.

Material properties

Temperature dependent physical and mechanical material properties, including thermal conductivity, coefficient of thermal expansion, specific heat, density, elastic modulus, yield stress and Poisson ratio, were measured in a previous investigation[16] and were used for both thermo-electrical and thermo-mechanical analysis. It should be noted that the mechanical properties of the aluminium alloy were kept unchanged beyond the temperature of 500°C up to melting of the alloy. Electrical resistance of the workpiece and electrode materials were obtained from Ref. 18 which are listed in Table 2. In this model, the contact resistances between the electrode/workpiece interface and workpiece/workpiece faying surfaces were considered and simulated by assigning temperature and pressure dependent resistance properties to one layer of elements along the contact interfaces, which had a thickness of 0·05 mm. The value of contact resistance (equivalent contact resistance) was estimated from Refs 19 and 20 as listed in Table 2. It

Table 2 Electrical resistance of aluminium alloy and estimated contact resistance between electrode/workpiece and workpiece/workpiece

	Temperature, °C				
	20	200	300	400	500
Aluminium alloy resistance, $\times 10^8$ Ω m	5·8	7·7	8·8	9·8	20·5
Copper electrode resistance, $\times 10^8$ Ω m	2·64	3·99	5·19	6·01	7·48
Contact resistance between electrode and workpiece, $\times 10^8$ Ω m	580	370	280	98	20·5
Contact resistance between workpiece and workpiece, $\times 10^8$ Ω m	290	190	140	49	20·5